O-induced modification of growth of thin Cu films on Ru(0001)

H. Wolter, K. Meinel, and Ch. Ammer
Martin-Luther-Universität Halle-Wittenberg, Fachbereich Physik, D-06099 Halle, Germany

K. Wandelt
Universität Bonn, Institut für Physikalische und Theoretische Chemie, D-53115 Bonn, Germany

H. Neddermeyer
Martin-Luther-Universität Halle-Wittenberg, Fachbereich Physik, D-06099 Halle, Germany

(Received 8 August 1996; revised manuscript received 12 May 1997)

The film growth of Cu on clean and O-precovered Ru(0001) substrates at temperatures between 300 and 450 K is studied by means of scanning tunneling microscopy. On clean Ru(0001), the Cu films grow in a multilayer mode. For an O precoverage, $(\Theta_O) < 0.1$ monolayer (ML), O remains trapped at the Cu/Ru interface and the Cu film grows similarly as on clean Ru(0001). Precovering the Ru(0001) substrate with more than 0.1 ML of O strongly modifies the film morphology. The excess O migrates to the surface of the growing film and acts as a surfactant. Domains of an O/Cu structure are formed, the lateral extension of which linearly increases with Θ_O. For $0.4 < \Theta_O \leqslant 0.5$ ML, the O/Cu structure covers the film surface completely. For $0.2 \leqslant \Theta_O \leqslant 0.5$ ML, a perfect layer-by-layer growth with a relatively high nucleation density is forced at temperatures around 400 K. Decreasing the temperature and/or Θ_O yields multilayer growth. For $0.4 < \Theta_O \leqslant 0.5$ ML, temperatures above 430 K, and substrate terrace widths below 100 nm, step-flow growth is observed. Two different types of O/Cu surfactant structures (A- and B-type) are identified. The A-type structure is established for $0.1 < \Theta_O \leqslant 0.4$ ML, and displays some ordering on a local scale (distorted hexagonal lattice). It causes heterogeneous nucleation at surface sites formed by a misfit-induced moiré-like relaxation of the Cu film. Its surfactant effect can be described by the concept of two mobilities, which is based on a low adatom mobility during nucleation, and a high adatom mobility on top of small islands. This implies an increase of the attempt rate of Cu adatoms for step descent, enhancing interlayer diffusion. The B-type structure is established for $0.4 < \Theta_O \leqslant 0.5$ ML, and contains a more irregular arrangement of O atoms. We assume that it behaves like a continuous O/Cu layer, on top of which the adatoms migrate. Its surfactant effect is attributed to a large diffusion barrier and a small additional step-edge barrier prevailing on top of the O/Cu layer. The latter also implies increased interlayer diffusion. The relationship of our results to previously observed work-function oscillations in the O-modified Cu film growth on Ru(0001) is discussed. [S0163-1829(97)00144-6]

I. INTRODUCTION

The deliberate manipulation of epitaxial film growth is a topical subject in thin-film research. One of the main objectives is the change of a three-dimensional (3D) growth mode into a layer-by-layer growth to attain a homogenous two-dimensional (2D) film morphology. The general possibilities of manipulating film formation may be derived from the initial stages of film growth, as has been demonstrated by Comsa and co-workers.[1,2] Epitaxial films are usually prepared under conditions far from equilibrium. Consequently, the film growth is controlled by kinetic processes. Initially, a nucleation phase occurs. The impinging atoms are thermally activated and migrate over the substrate surface until they meet and form stable nuclei. The density of nuclei quickly reaches saturation. The nuclei develop into small 2D islands, which grow by trapping adatoms at edge sites where the bonding is strong. With the island size increasing, a growing number of atoms directly impinges on the top of the islands. The latter atoms may jump over the step edge, migrating downward to the lower surface level into step sites. In this case, the film grows in a 2D mode by alternating nucleation, growth, and coalescence of 2D islands. If the atoms are partially captured on top of the islands by an additional energy barrier at the step edge,[3,4] the atoms nucleate on top of the islands before the already existing islands coalesce. As a consequence, islands are repetitively created on top of previously formed islands and the film grows in a 3D multilayer mode.[5–7] Hence, the decisive process determining the growth mode is the interlayer mass transport downward over the step edges. To induce a perfect 2D layer-by-layer growth, one has to intensify the interlayer diffusion. Generally, there are two possibilities for managing that. (i) By increasing the number of approaches to steps (on the upper terrace), the atoms will more likely jump over the steps before they are trapped by nucleation. (ii) The probability of descent will be increased by decreasing the additional step-edge barrier. (i) can be realized by an artificial decrease of the mobility of adatoms in the nucleation stage, leading to an increase of the nucleation density, which is accompanied by a decrease of island size (concept of two mobilities[1]). Atoms impinging on smaller islands can more frequently visit the step edges, which increases the probability of jumping over the step. This may induce the growth of 2D islands until coalescence. In order to maintain a continued layer-by-layer growth, one has to repeat the artificial nucleation after completion of each layer.

0163-1829/97/56(23)/15459(12)/$10.00 © 1997 The American Physical Society

This can be attained by a temporary temperature reduction and/or by jumps of the deposition rate,[8,9] both of which very effectively increase the nucleation density according to nucleation theory.[10,11] Moreover, the nucleation density can be increased by periodic ion sputter pulses, which create additional adatoms, thus enhancing the nucleation.[9]

All these kinds of growth manipulation, however, require great efforts in growth control and preparation. Fortunately, growth can also be influenced by reducing the additional step-edge barrier, which directly leads to a layer-by-layer growth. This has been demonstrated for Pt/Pt(111) homoepitaxy.[6] In Ref. 6, 2D film growth was initiated by simply reducing the temperature, which, in the case of Pt(111), induces a decrease of the additional step-edge barrier by changing the island morphology. The step-edge barrier can also be manipulated by applying surfactants, i.e., small amounts of a foreign material floating up into the surface layer of the growing film.[12] In metal epitaxy, this was studied in detail for the Ag/Ag(111) system by using Sb as a surfactant.[13–15] However, the surfactant effect of Sb is a complex phenomenon, as has been revealed by scanning tunneling microscopy (STM).[15] Sb not only reduces the additional step-edge barrier, but it also increases the diffusion barrier for Ag adatoms on terraces and at step edges. This leads to a high density of 2D Ag islands of dendritic shape possessing a high number of step sites. Hence, the 2D film growth is also affected by an increased number of attempts of Ag atoms to descend from the islands. The same complexity may be expected for O, which has been identified as another very effective surfactant in metal epitaxy. O-induced layer-by-layer growth has been reported for Pt/Pt(111),[16] Cu/Ru(0001),[17] Cu/Pt(111),[18] and Cu/Cu(111).[2] The O-mediated growth effects have been investigated mainly by integral methods. Detailed real-space investigations of the film morphology have been sparse up to now. Therefore, the role of O as a surfactant is not yet fully understood.

In the present work, we have re-examined both the conventional and the O-modified growth of Cu films on a Ru(0001) substrate by means of STM. The conventional growth of clean Cu films on hexagonal-closed-packed (hcp) Ru(0001) has been extensively investigated as a model system of heteroepitaxy of strained thin metal films.[19–21] The lattice parameter of Cu in the Cu(111) surface is 5.5% smaller than that of Ru(0001). Due to the relatively large misfit, the Cu film grows by the Stranski-Krastanov mode (2D film growth followed by 3D island formation) at temperatures above 500 K.[19] At temperatures between 300 and 500 K, the growth is kinetically controlled and proceeds via 3D multilayer island growth. Due to the high mobility of Cu adatoms, the nucleation density is relatively small, which induces the growth via step flow on small terraces. The first layer grows to a pseudomorphic structure. The film stress is reduced by a series of reconstructions in the following layers, as has been demonstrated by the STM investigations of Günther *et al.*[20] Above 3 monolayers (ML), the Cu film grows with the lattice parameter of clean Cu(111) in a face-centered-cubic (fcc) structure, with the Cu layers almost completely relaxed. The films, however, are slightly rotated by about $\pm 0.65°$ with respect to the substrate[21] and show a moiré corrugation pattern corresponding to the Cu/Ru misfit, which is of nearly perfect long-range order at temperatures above 450 K.

Small amounts of O drastically modify the Cu film formation. For an O precoverage $(\Theta_O) > 0.1$ ML of the Ru(0001) substrate, part of O floats to the surface of the growing Cu film, as has been demonstrated by Auger electron spectroscopy[22] (AES) and ion-scattering spectroscopy.[23] This reduces the stability of the kinetically grown Cu films and lowers the temperature, where the transition from multilayer growth to Stranski-Krastanov growth occurs.[24] Moreover, the O induces a layer-by-layer mode of film growth under special preparation conditions. The latter was proved by *in situ* monitoring of the integral work function during Cu film growth.[17] Work-function oscillations with a ML period were observed at substrate temperatures around 400 K, if Ru(0001) was precovered with 0.3–0.4 ML of O. For other values of Θ_O, only a continuous change of the work function to a steady-state value occurred. The work-function oscillations allowed the conclusion to be drawn that the interaction of O with Cu on the surface induces a layer-like growth of Cu on Ru(0001) with a periodic variation of step density.[17] In principle, these results and their interpretation are confirmed by a recent study of Cu growth on Cu(111), using thermal-energy He atom scattering (TEAS).[2] For special O doses and temperatures of 200 and 400 K, respectively, slight oscillations of TEAS intensity were observed. In Ref. 2, the surface O is concluded to reduce the mobility of Cu adatoms, resulting in an island density higher than that of the pure Cu/Cu(111) system. This is in accordance with previous STM investigations of the Cu/O/Ru(0001) system, indicating that O induces a high island density in the first Cu layers grown at room temperature (RT).[25]

The aim of our STM investigations was to characterize the O-modified Cu film growth on Ru(0001) in more detail for substrate temperatures between 300 and 450 K. Our experiments cover the entire range of Θ_O accessible under ultrahigh vacuum $(0 \leqslant \Theta_O \leqslant 0.5$ ML).[26] Three different growth regimes were revealed that strongly depend on temperature and Θ_O. With the temperature rising, these are 3D multilayer growth (300–360 K), 2D layer-by-layer growth (360–430 K), and step-flow growth (430–450 K). The investigations confirm the O-induced increase of the nucleation density suggested in previous experiments.[17] At $\Theta_O \approx 0.1$ ML, first traces of O are detected in the surface of the Cu film. Domains of an O/Cu structure are observed, the lateral extension of which linearly increases with Θ_O. For $0.4 < \Theta_O \leqslant 0.5$ ML, the growing Cu film is completely covered with an O/Cu layer.

Two different O/Cu surfactant structures (named A- and B-type) have been identified. The A-type O/Cu structure is established for $0.1 < \Theta_O \leqslant 0.4$ ML. Locally, it displays some ordering in the form of a distorted hexagonal lattice. It causes heterogeneous nucleation at special surface sites formed by the misfit-induced moiré-like relaxation of the clean Cu film. Triangular islands develop within the O/Cu domains, the edges of which run along [110]-like directions. Small islands remain free of O. The diffusion length of Cu adatoms on top of the O-free islands is larger than on the O/Cu domains. This implies a high attempt rate for step descent of Cu adatoms, which drastically increases interlayer

diffusion. The B-type O/Cu structure is established at $0.4 < \Theta_O \leq 0.5$ ML, containing more irregularly arranged O atoms. It completely covers the Cu film. We assume that it behaves like a continuous layer, on top of which the Cu adatoms migrate. For the B-type structure, the surfactant effect is ascribed to a large diffusion barrier and a small additional step-edge barrier established at the O/Cu layer, which implies a stronger interlayer diffusion. Our STM investigations are discussed in relation to previous work-function measurements.

The paper is arranged as follows. The experimental details are outlined in Sec. II and the results are given in Sec. III. The discussion of the results follows in Sec. IV. Finally, the main results of our investigations are summarized in Sec. V.

II. EXPERIMENT

The experiments were performed in an ultrahigh-vacuum chamber with an ion getter pump (base pressure 5×10^{-11} mbar), equipped with an STM operating at RT. This microscope consists of a piezoelectric tripod for xyz translation of the tip, and a piezoelectric stepper with the sample carrier. The tip was electrochemically etched from a W wire. Details of the construction are described elsewhere.[27] The STM was used in the constant-current mode with typical sample bias voltages U, in the range between -50 mV and -1 V, and a tunneling current I on the order of a few nA. The chamber also houses instrumentation for high-resolution low-energy electron diffraction (LEED).

The Ru(0001) crystal of a miscut of less than 0.5° was mounted on a transfer plate of Mo and prepared by cycles of Ar ion bombardment (energy: 1 keV, current density: about 10 μA/cm^2) followed by heating to 1300 K, each step lasting for half an hour. After this initial treatment there followed cycles of 20 Langmuir (L) ($1 \text{ L} = 1.33 \times 10^{-6}$ mbar s) of O adsorption and desorption by heating to 1600 K to remove C and S contaminants from the surface, as described elsewhere.[24,28] Sample heating was performed by electron bombardment and radiative heating via a W filament on the backside of the crystal. Initially, the temperature was measured by a Ni/NiCr thermocouple spot welded to the edge of the crystal. After calibrating the heating parameters the thermocouple was cut off to allow the free sample transfer to the STM by means of a wobble stick. The cleanness of the sample was checked by LEED and STM. The final surface showed an intense and clear 1×1 LEED pattern. The STM images revealed large clean terraces, typically about 100 nm in width. Under stable tip conditions, the Ru(0001) surface and the Cu(111) film were acquired with atomic resolution.

In the growth experiments, O was dosed via a leak valve at a constant pressure of 2×10^{-9} mbar at a substrate temperature of 400 K. The Cu films were prepared by molecular-beam epitaxy. Cu of 99.996% purity was evaporated from a resistively heated W basket. The temperature of the basket was controlled by an encapsulated Ni/NiCr thermocouple. During evaporation the pressure increased to about 1×10^{-10} mbar. The evaporation rate of typically 0.2 ML/min was determined by a quartz oscillator. The rate was cross checked by imaging the areas covered with ultrathin 2D Cu layers using STM. In determining the Cu coverage, we estimated an error of about 10%. For each experiment, the clean Ru(0001) surface was restored by desorbing Cu and O by heating the crystal to 1600 K.

Since the Cu film growth strongly depends on the quantity of preadsorbed O, it was important to reliably determine Θ_O. Using O-induced intensity changes in the LEED pattern,[26] previous work-function measurements, in combination with AES,[24,28] and the known coverage for a certain surface structure[29,30] enabled us to calibrate our O_2 dose scale. In particular, we used the fact that at 400 K O_2 adsorbs dissociatively, developing a $p(2\times2)$ overlayer structure up to $\Theta_O = 0.25$ ML, and a $p(2\times1)$ overlayer up to a saturation coverage of 0.5 ML.[29,30] A characteristic increase of curvature of the work-function rise was observed if the $p(2\times2)$ was completed.[26,28] Simultaneously, a sharp intensity maximum in the $p(2\times2)$ LEED spots was measured.[26] We used both signatures of the completion of the $p(2\times2)$ to determine our dose calibration. We followed the course of the $p(2\times2)$ LEED spot intensity during the O_2 exposure to find the sharp intensity maximum. This allowed us to correlate our dose scale and the observed surface structures with previous work-function measurements.[26,28] The accuracy of determining the O coverage was estimated to be better than 10%. More details of this calibration are described in another paper,[31] which focuses on the evolution of the O structures on Ru(0001), revealed by STM.

III. RESULTS

A. Conventional Cu/Ru(0001) film growth

First, the conventional growth of thin Cu films on clean Ru(0001) is considered. The Cu/Ru(0001) system was already analyzed in detail by the Behm group[20] using STM at growth temperatures above 500 K. Different relaxation structures depending on film thickness were detected. Our investigations focus on the Cu film formation on Ru(0001) at temperatures between 300 and 450 K in order to provide a reference for the O-mediated Cu film growth. In particular, results are presented for the high coverage regime (>3 ML) of Cu/Ru(0001), where the Cu films are almost completely relaxed. The STM images of Fig. 1 present typical film morphologies. Figure 1(a) shows a 10-ML-thick Cu film grown in the 3D multilayer mode at 300 K. About five layers grow simultaneously with a relatively small number of 2D nuclei or islands having a density of about 2×10^{10} cm^{-2}. Similar growth structures and island densities are observed at temperatures around 400 K indicating a weak temperature dependence of the nucleation.

Figure 1(b) shows a 20-ML-thick Cu film grown at 450 K. The film morphology is strongly changed. The film displays large plateaus with smooth surfaces separated by deep holes. In the holes the local Cu film thickness is 2–3 ML, which we deduced from characteristic relaxation structures of 2- and 3-ML-thick Cu films on Ru(0001) (Ref. 20) [not visible in Fig. 1(b) due to the gray-tone scale chosen]. The measurement demonstrates the transition to the Stranski-Krastanov growth of the Cu/Ru(0001) system, as has been revealed for temperatures above 500 K.[19]

The STM images of Fig. 1(c) show a 6-ML-thick Cu film prepared at 400 K, measured with high resolution. Linear

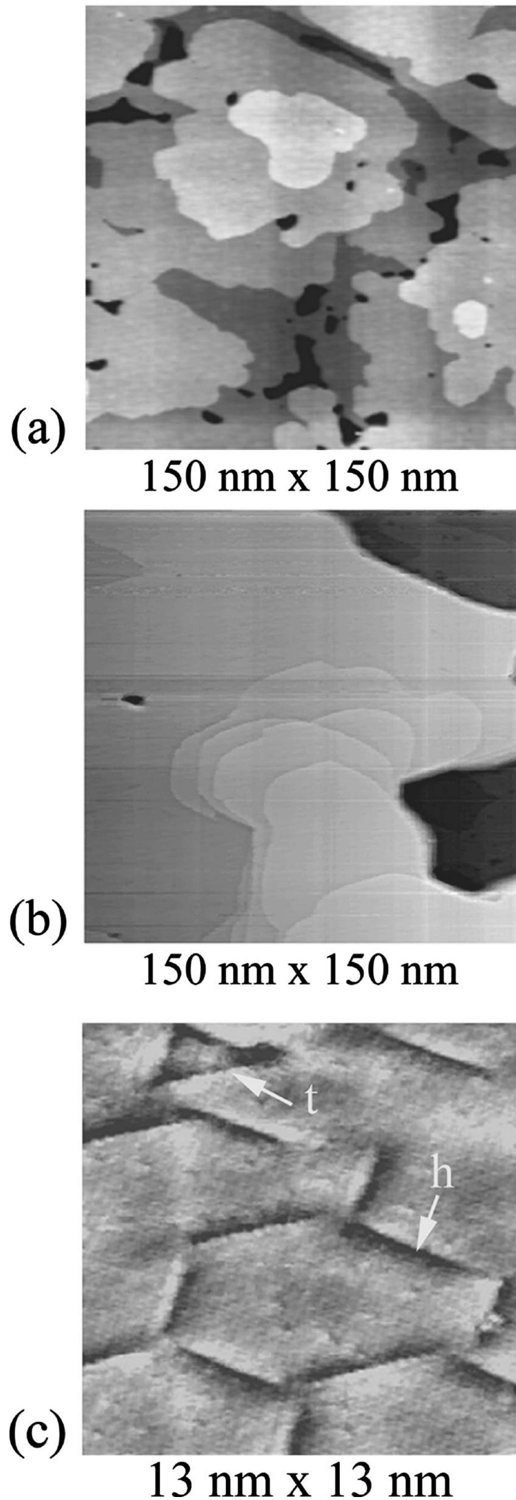

FIG. 1. STM images of Cu films grown on clean Ru(0001). (a) Growth temperature 300 K, film thickness about 10 ML; (b) growth temperature 450 K, film thickness about 20 ML; and (c) growth temperature 400 K, film thickness 6 ML. (a) and (b) display variants of the 3D film morphology; (c) shows characteristic patterns of triangular defects (t) and honeycomblike defects (h) in high resolution belonging to a moiré-like reconstruction of the Cu film.

defects are observed that give rise to a marked bright/dark contrast. They are about 4 nm long and run parallel to [110]-like directions. The bright and dark regions of the linear defects are measured at about 0.2 nm above and below the mean surface level. They form either triangles (t) or elements of a honeycomb pattern (h). We observe these defects at growth temperatures between 300 and 450 K and a film thickness between 5 and several tens of ML. They are parts of misfit-induced metastable relaxation structures of the Cu film, which are preforms of the stable moiré structure occurring at temperatures >450 K, having a film thickness >3 ML. Usually, the moiré-like relaxation structures are strongly disturbed and only of short-range order. Respective details will be described in a separate paper.[32] Most interesting are the triangular defects, having a density of about 3×10^{12} cm^{-2} at growth temperatures around 400 K. As discussed below, they may drastically influence the O-mediated Cu film growth under certain preparation conditions.

B. O-mediated Cu/Ru(0001) film growth as a function of Θ_O

O-mediated Cu film growth on Ru(0001) has been systematically analyzed as a function of Θ_O and growth temperature. We first characterize the film morphology, which develops with rising Θ_O at a constant growth temperature of 400 K, where the O-induced layer-by-layer growth was previously observed.[17] In the investigations, the film thickness was nominal 6.4 ML. First, the general features of the O-induced modifications of the Cu film morphology are considered, which are illustrated by large-scale STM images (Figs. 2 and 3). Then, high-resolution STM images show the details of O-induced structures on top of the growing Cu films.

For $0<\Theta_O<0.1$ ML, the Cu film morphology was almost the same as in conventional Cu film growth, with no indication of O in the surface layer (not reproduced). This is in agreement with previous investigations,[22] which revealed that about 0.1 ML of O remains trapped at the Cu/Ru interface.

At $\Theta_O\approx0.1$ ML, the film morphology starts to change, as the STM image of Fig. 2 shows for $\Theta_O=0.12$ ML. The multilayer growth mode is still operative. About 5 layers are growing simultaneously. Some parts of the top terraces, however, are occupied by a large number of small Cu islands at a local density of about 2×10^{12} cm^{-2} (see arrow). Below,

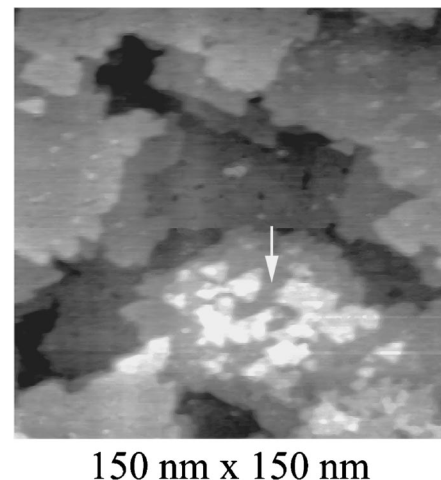

FIG. 2. STM image of a 6.4-ML-thick Cu film grown at 400 K on slightly O-precovered Ru(0001) showing multilayer growth ($\Theta_O=0.12$ ML). For details see text.

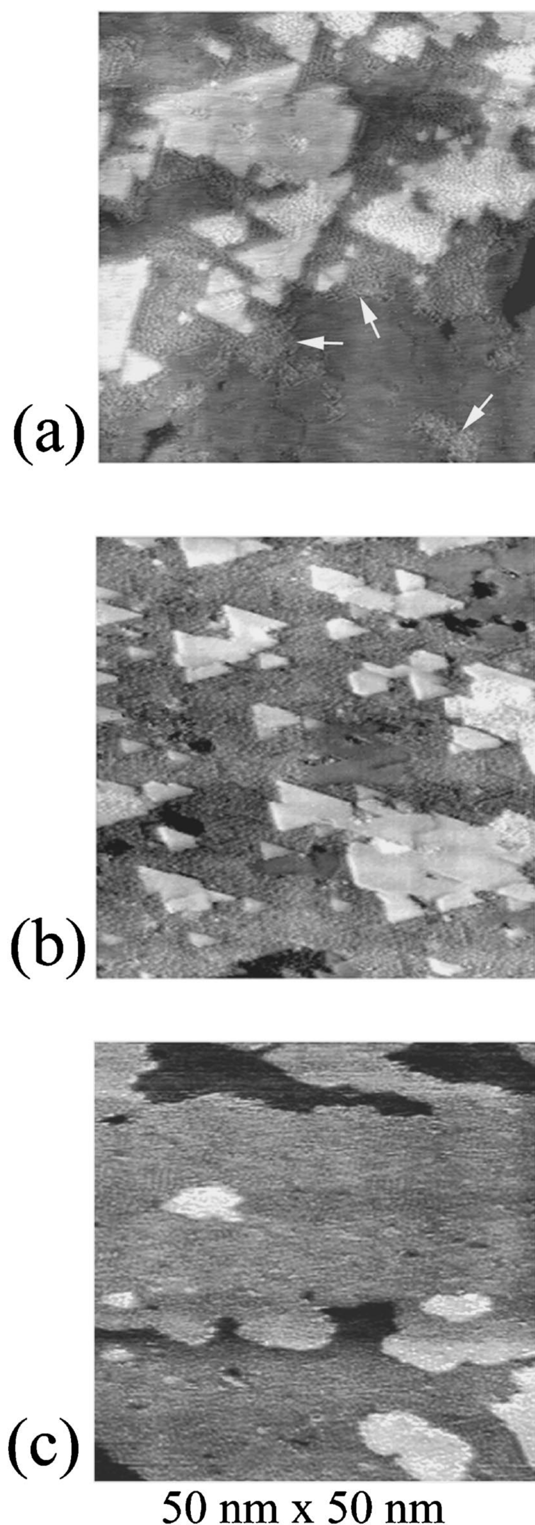

FIG. 3. STM images of 6.4-ML-thick Cu films grown at 400 K revealing layer-by-layer growth for (a) Θ_O=0.2 ML, (b) Θ_O=0.32 ML, and (c) Θ_O=0.42 ML. The arrows in (a) indicate areas of the O/Cu surfactant structure. There is a clear contrast between these areas and the O-free neighborhood.

it will be shown that these islands are formed within areas showing a characteristic corrugation pattern, which is induced by an O/Cu surfactant structure (not resolved in the large scale image of Fig. 2).

Increasing Θ_O to 0.2 ML induces an almost perfect layer-by-layer Cu film growth [Fig. 3(a)]. Even if large film areas (μm range) are inspected by a number of STM images, we observe only 1–2 simultaneously growing layers. The film formation is governed by a high density of nuclei and islands, respectively. The Cu islands are of triangular shape, with step edges parallel to [110]-like directions. Similarly to Fig. 2, the film surface is rather inhomogeneous. There are areas with a high density of islands and others entirely free of islands. The islands strongly differ in size. Larger islands are usually surrounded by smaller ones, yielding a large size distribution.[33] The surfaces of smaller islands are generally very smooth, as expected for clean Cu. Around the islands, there are highly corrugated areas (maximum corrugation height 0.06 nm) as in the former experiment. In the STM image of Fig. 3(a), the resolution is just sufficient to perceive the roughness of these areas. The corrugated areas occur on smooth Cu terraces (arrows) and, occasionally, on large islands, too. The smooth terraces appear about 0.03 nm below the maximum height of the corrugated areas, showing the defects of the misfit-induced moiré-like reconstruction of the Cu film, as Fig. 1(c) indicates in high resolution.

Increasing Θ_O from 0.12 to 0.2 ML increases the coverage of the corrugated areas. In Fig. 3(a), the latter cover about 40% of the surface. Cu nuclei and islands only occur within the corrugated areas. Therefore, we conclude that the corrugated areas correspond to domains of an O/Cu surfactant structure, which strongly increases the nucleation. Within the O/Cu domains there is a nucleation density of about 2×10^{12} cm^{-2} that is similar to that locally observed at Θ_O=0.12 ML (Fig. 2, arrow). The height of the smooth Cu islands (within the O/Cu areas) above the smooth Cu terraces was determined to be 0.20 nm, which corresponds to the monolayer height of 0.208 nm of Cu(111). Hence, we conclude that the Cu islands are located within the O/Cu structure and not on top of it.

In Fig. 3(b), the STM image of a Cu film demonstrates that the almost perfect 2D mode of film growth is preserved at Θ_O=0.32 ML. A total Cu nucleation density of about 2×10^{12} cm^{-2} is measured. The rough O/Cu domains, now cover about 80% of the Cu film. Only small areas still display the O-free Cu surface. Within the O/Cu domains, the number of triangular islands is similar to that observed in Fig. 3(a). The island size is more homogeneous than in Fig. 3(a). Again, small islands exhibit a smooth surface. The characteristic defects of the Cu film, shown in Fig. 1(c), are partly resolved on terraces and large islands.

For Θ_O=0.40 ML, the film surface is almost completely covered with the O/Cu structure and the nucleation density reaches a maximum of about 2.5×10^{12} cm^{-2}. As high resolution images will reveal below, small islands and the edges of larger islands remain free of the O/Cu structure.

The STM image of Fig. 3(c) demonstrates the film growth occurring at Θ_O=0.42 ML. Surprisingly, the small increase of Θ_O from 0.40 to 0.42 ML strongly changes the film morphology. The film growth continues in the layer-by-layer mode. However, the nucleation density is drastically reduced by a factor of almost 30. Nevertheless, it is a factor of about 10 larger than for the conventional Cu film growth at 400 K. The shapes of the Cu islands also change, becoming irregular and more compact. Most conspicuously, the whole film sur-

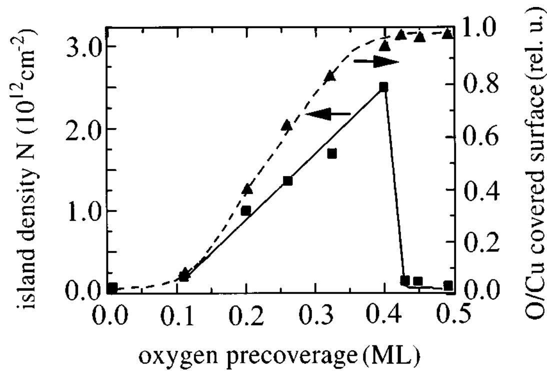

FIG. 4. Nucleation density (solid line) and surface coverage (dashed line) of the O/Cu surfactant layer, as measured for the O-modified Cu film growth on Ru(0001) at 400 K as a function of Θ_O.

face including small Cu islands and island edges is now covered with a rough O/Cu structure. This characteristic change of the film morphology at $\Theta_O = 0.40 \pm 0.02$ ML, has been proven for different Cu film thickness in a series of experiments.

Further increasing Θ_O up to the saturation at 0.5 ML does not induce a further change in the film morphology. Again, a layer-by-layer morphology occurs, with island shapes and densities similar to that in Fig. 3(c).

Inspecting different growth stages (e.g., island formation and coalescence) at film thicknesses between 5 and 20 ML,[33] we conclude that the ratio between the smooth areas of clean Cu and the rough ones of the O/Cu domains remains constant for any Θ_O value. Hence, the surface coverage of the O/Cu structures is independent of film thickness and growth stage, which corresponds to the results of previous AES investigations.[22]

Figure 4 summarizes the main data hitherto obtained, with the nucleation density and the surface coverage of the rough O/Cu domains measured at 400 K as a function of Θ_O. At $\Theta_O \approx 0.1$ ML, small O/Cu domains start to appear on the Cu film surface, with the island density beginning to deviate from that of the conventional Cu film growth on Ru(0001). At $0.1 < \Theta_O < 0.4$ ML, the relative surface coverage of the O/Cu domains increases almost linearly. Correspondingly, the average nucleation density increases linearly up to a maximum of about 2.5×10^{12} cm^{-2}. In that range of Θ_O, the number of Cu nuclei created within the O/Cu domains is constant. At $\Theta_O = 0.42$ ML, the nucleation density drastically drops to about 1×10^{11} cm^{-2}. This sudden decrease in nucleation occurs whenever the O/Cu structure completely covers the film surface. Further increasing Θ_O does not induce further changes in nucleation and O/Cu structure.

The rapid decrease in the nucleation density at $\Theta_O = 0.42$ ML is most conspicuous. Therefore, we conclude that there are two different types of O/Cu structures, strongly differing in nucleation efficiency. In the following, the structure with the high nucleation efficiency formed at $0.1 < \Theta_O \leq 0.4$ ML will be called A-type structure and that with the low nucleation efficiency formed at $0.4 < \Theta_O \leq 0.5$ ML B-type structure.

Both O/Cu structures are shown in the high-resolution images of Fig. 5. The images were taken of 6.4-ML-thick Cu films grown at 400 K, with $\Theta_O = 0.32$, 0.40, and 0.5 ML. Both types of O/Cu structures are characterized by characteristic patterns of small protrusions and depressions. Actually, there are several structural and morphological differences that support the idea of two different O/Cu surfactant structures. Considering the A-type structure, we observe a certain order on a local scale. Typically, a distorted hexagonal lattice, as shown in Fig. 5(a), is formed in A-type O/Cu domains, with unit mesh dimensions of about 0.53 and 0.66 nm, respectively. However, there is no long-range order and, consequently, no O-induced LEED pattern. Furthermore, the bright area in Fig. 5(a) demonstrates that islands growing within the A-type structure initially remain free of O. Even at $\Theta_O = 0.40$ ML where the A-type structure almost completely covers the film surface [Fig. 5(b)], smooth surfaces of clean Cu are observed for small islands (i). This also holds for the edges of larger islands. In contrast to that, the B-type structure always completely covers the Cu film surface, including even small islands and island edges, as demonstrated in Fig. 5(c). For the B-type structure, the degree of order is somewhat lower. In the STM images, the O-induced corrugations are more irregularly arranged (cf. the images in Fig. 5). In addition, the B-type structure seems to be more dense with respect to the O-induced corrugation.

Comparing the film morphology in Figs. 5(a)–5(c) induced by both O/Cu structures, it is very characteristic for the A-type structure that small Cu islands are of triangular shape with steps running parallel to [110]-like directions. For the B-type structure, the islands are of irregular shape, with no step direction prevailing. In addition, defects being part of the moiré-like relaxation of the Cu film [cf. Fig. 1(c)] are clearly discernible within the A-type structure. Figure 5(b) shows a part of a film with honeycomblike defects (h) formed within an A-type O/Cu domain. The A-type O/Cu structure seems to be interrupted at the defects, which accentuates their visibility. It is most characteristic that we only observe honeycomblike defects within the O/Cu domains, whereas the triangular defects (t) exclusively occur on the O-free areas. Obviously, the smallest triangular islands (i) are always of the same shape and dimensions as the triangular defects of clean Cu films. Moreover, the local density of the small islands is almost the same as that of the triangular defects. This correlation of triangular islands (i) and defects (t) is also reflected in the maximum nucleation density measured if the A-type O/Cu structure almost completely covers the film surface. At 400 K, it is 2.5×10^{12} cm^{-2}, which is comparable to the density of triangular defects (3×10^{12} cm^{-2}) on clean Cu films.

As mentioned above, the B-type structure always completely covers the whole surface; thus it can be considered as a continuous layer that is not interrupted at the defects of the Cu film. The defects of the moiré-like reconstruction are therefore hard to detect, and the film surface appears more homogeneous.

C. O-mediated Cu/Ru(0001) film growth as a function of temperature

We now turn to the temperature dependence of the O-mediated Cu film growth. In particular, we will show the difference in the temperature dependence of the Cu nucleation of both O/Cu structures. For analyzing the A-type O/Cu

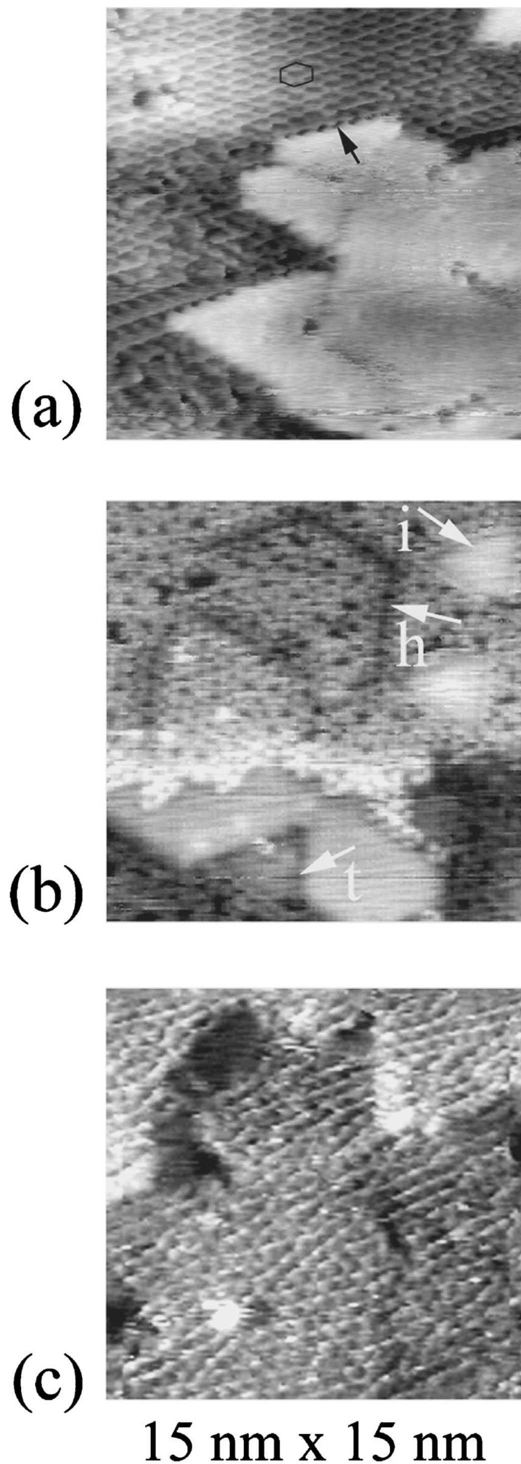

FIG. 5. High-resolution STM images of Cu films grown on O-precovered Ru(0001). (a) Θ_O=0.32 ML, (b) Θ_O=0.40 ML, and (c) Θ_O=0.5 ML. (a) and (b) show the *A*-type O/Cu surfactant structure; the smooth areas belong to O-free islands or island edges, respectively. (c) shows the *B*-type O/Cu surfactant structure. All films have a nominal thickness of 6.4 ML and are grown at 400 K. For details see text.

structure, we use an O precoverage of 0.32 ML, where almost 80% of the surface is covered with the *A*-type O/Cu structure during Cu film growth [cf. Figs. 3(b) and 4]. Figure 6 shows STM images of 6.4-ML-thick Cu films grown with Θ_O=0.32 ML at RT and 400 K, respectively. At RT [Fig. 6(a)], the film growth proceeds in the multilayer mode, characterized by small atomically stepped growth hillocks of 3 to 4 incomplete layers. At 400 K, however, we observe layer-by-layer growth. At both temperatures, the films are covered with domains of the *A*-type structure (not resolved in Fig. 6). Small O/Cu domains are observed at RT, because the *A*-type O/Cu structure is interrupted at the step edges of the hillock terraces. Most conspicuously, the density of the Cu islands of about 5×10^{11} cm^{-2} is smaller by a factor of about 3 than that observed at 400 K. This result is rather surprising, as the nucleation density is expected to increase with decreasing temperature.

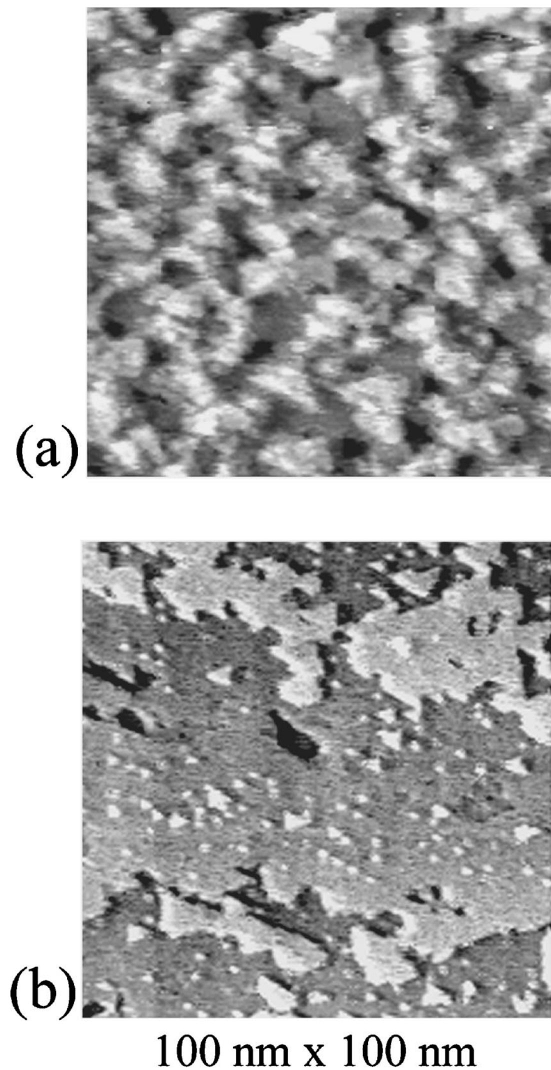

FIG. 6. STM images of 6.4-ML-thick Cu films grown on Ru(0001) at temperatures of (a) 300 K and (b) 400 K, with Θ_O=0.32 ML, revealing (a) multilayer growth and (b) layer-by-layer growth.

To investigate the temperature dependence of the Cu film growth mediated by the *B*-type O/Cu structure, we use the O-saturated Ru(0001) substrate (Θ_O=0.5 ML). Figure 7 shows STM images of Cu films of a mean thickness of 6.4 ML, grown at 330, 380, and 450 K. At 330 K, the growth proceeds in the multilayer mode [Fig. 7(a)]. A relatively high nucleation density of about 2×10^{12} cm^{-2} is observed, causing the formation of a large number of small, atomically stepped, growth hillocks. About five atomic layers are simul-

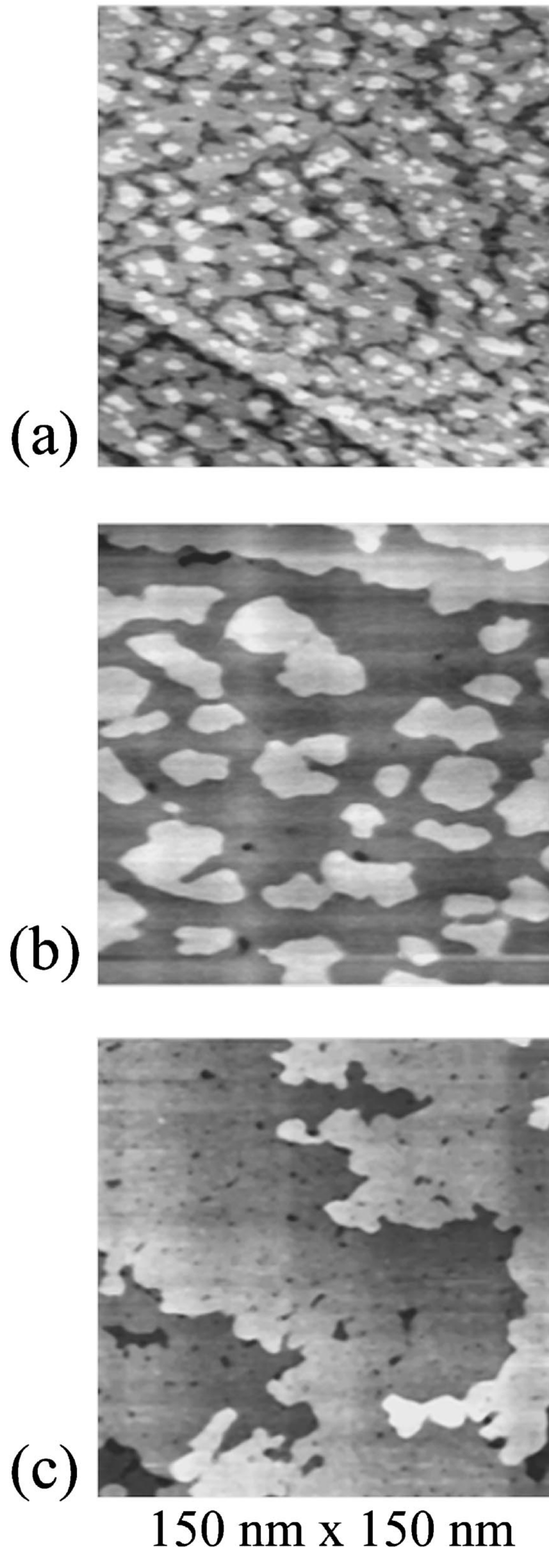

FIG. 7. STM images of 6.4-ML-thick Cu films grown on an O-saturated Ru(0001) substrate (Θ_O=0.5 ML) at temperatures of (a) 330 K, (b) 380 K, and (c) 450 K. The measurements reveal (a) multilayer growth, (b) perfect layer-by-layer growth, and (c) step flow.

taneously growing. Figure 7(b) demonstrates the O-induced layer-by-layer growth at 380 K as described above, governed by an island density of about 2×10^{11} cm^{-2}. Figure 7(c) demonstrates the growth by step flow at 450 K. At that tem-

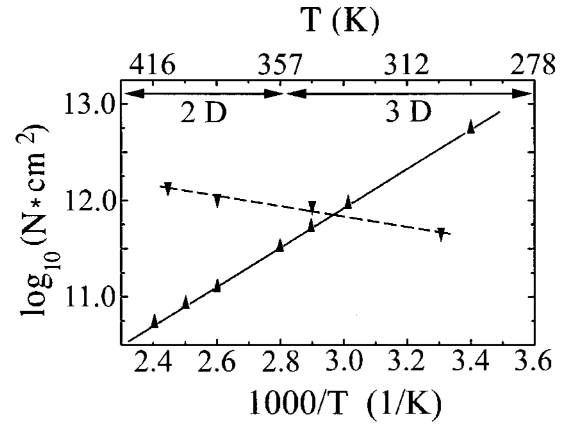

FIG. 8. Arrhenius plot of nucleation density, as measured by STM for Cu film growth on Ru(0001) at different temperatures on O-precovered Ru(0001). O precoverage: 0.32 ML (▼) and 0.5 ML (▲). The temperature ranges of the observed growth modes are indicated.

perature, 2D nucleation and island growth, respectively, are observed solely on terraces >100 nm, with a rather low island density of about 1×10^{10} cm^{-2}. On our Ru crystal, with a mean terrace width of 100 nm, step flow dominates over 2D island growth at temperatures above 430 K. In all examples, the film surface is entirely covered with the B-type O/Cu structure similar to that displayed in the high-resolution image of Fig. 5(c).

The measured dependencies of island density N versus growth temperature are presented in the Arrhenius plot of Fig. 8. The dashed and full lines connect the data points obtained for Cu films covered with either the A-or B-type O/Cu surfactant structure, respectively. The ranges of the different growth modes observed are indicated. For the B-type O/Cu structure, there is a strong temperature dependence of the nucleation density, revealing an Arrhenius-like behavior. The island density changes by two orders of magnitude within the temperature range investigated (300–450 K). Most obvious, however, is the reversed temperature dependence of the nucleation density measured for the A-type O/Cu structure.

IV. DISCUSSION

A. Conventional Cu film growth on clean Ru(0001) ($\Theta_O=0$)

As Fig. 1 shows, the low island density of the clean Cu films and its weak temperature dependence at temperatures between 300 and 400 K indicate a high mobility of Cu adatoms on clean Cu(111) films. This agrees with previous experimental and theoretical investigations[2,34,35] revealing a small diffusion barrier E_d of 0.03–0.05 eV for the Cu adatoms on Cu(111) crystal surfaces.

The observed multilayer growth of Cu on clean Ru(0001) demonstrates that the interlayer diffusion is hampered by an additional step-edge barrier Δ_s (Δ_s is defined by $\Delta_s=E_s-E_d$, with E_s being the energy barrier of the step descent). Δ_s can be roughly estimated by applying a formalism of multilayer growth, presented recently by Meyer *et al.*[7] It was applied to conventional and Sb-mediated Ag(111) homoepitaxy.[7] For Δ_s, the formalism yields

$$\Delta_s \approx kT \ln\{[(D/2R_1)^2 - h_f/h_i]R_1/2a_0\}, \quad (1)$$

where D is the average distance between islands grown on a smooth substrate, R_1 is the critical radius of the islands on top of which nucleation starts, and a_O denotes the lattice constant. h_f and h_i are the hopping rates of adatoms on the smooth film surface and on top of the islands, respectively. For our almost completely relaxed Cu films (mean thickness >6 ML), we assume $h_f = h_i$. We have utilized experiments, where Cu films of the Stranski-Krastanov morphology were prepared (growth temperature 550 K), displaying smooth plateaus (height >20 ML) larger than that in Fig. 1(b). The latter were used as substrates for investigating the Cu(111) homoepitaxy at RT (not shown). In the submonolayer region, we observed Cu islands of monatomic height on the Cu plateaus, and the beginning of formation of second layers on top. From the average island distance ($D \approx 250$ nm) and the critical radius of the second-layer formation ($R_1 \approx 50$ nm), respectively, we estimate an additional step-edge barrier of about 0.16 eV using Eq. (1). This value is in good agreement with previous estimates for similar systems such as Ag/Ag(111) and Pt/Pt(111).[7]

B. Growth for $0.1 < \Theta_O \leq 0.4$ ML

Precovering the Ru(0001) substrate with O drastically changes the film morphology. For $\Theta_O > 0.1$ ML, O/Cu surfactant structures are observed on top of the growing Cu film, which induce a perfect layer-by-layer growth for $\Theta_O > 0.2$ ML. First, we discuss the effects caused by the A-type O/Cu structure ($0.1 < \Theta_O \leq 0.4$ ML) and focus on the atomic arrangements within that structure. The STM images [Figs. 5(a) and 5(b)] reveal a distorted hexagonal pattern formed by depressions, with unit mesh dimensions of 0.53 and 0.66 nm, respectively. The arrangement of depressions is qualitatively similar to that observed by Jensen *et al.*[36] for O_2 adsorption on Cu(111). The authors identified a distorted hexagonal structure, of similar lattice parameters and two different supercell structures, called ''29'' and ''44'' structures. However, we detected neither these supercell structures in our STM investigations, nor any O-induced diffraction pattern by LEED. The latter indicates that the ordering of the O/Cu surfactant structure is only of short range and different from that observed for the adsorption of O_2 on Cu(111).[36] The atomic arrangements forming the O/Cu structures observed in our experiments are unknown up to now. They cannot be directly deduced from the STM images. There might be a mixture of topographic and chemical contrasts due to the complexity of the O/Cu system. For example, the depressions can be interpreted either as holes[36] within an O/Cu structure, or as individual O atoms.[37] Certainly, the O/Cu structures will correspond not only to simple adsorption layers of O atoms. We assume a kind of a surface oxide to be formed on the Cu film. This we conclude from combined LEED and STM investigations,[38,39] where we studied the O/Cu top layer formation on Cu films induced by preadsorption and postadsorption of O. At temperatures above 500 K, we observed O/Cu structures with long-range order, which we characterized by LEED. We have developed models of these structures, which consist of sandwichlike arrangements of $Cu_2O(111)$ layers.[39]

We now turn to the growth effects caused by the A-type structure. For $\Theta_O \geq 0.2$ ML, there is an almost perfect layer-by-layer growth at 400 K. The film growth is governed by a high density of O-free small islands. Surprisingly, the island density increases with increasing temperature. The nucleation and Cu island formation induced by the A-type structure will be discussed first. Within the O/Cu domains there are small triangular Cu islands, whose dimensions and local densities correspond to those of the triangular defects of the moiré-like relaxation of the Cu film [Fig. 5(b)]. This conspicuous correlation can be explained by the heterogeneous nucleation of Cu atoms within the triangular defects. The details of this mechanism of nucleation will be discussed in a special paper.[40] Here, we only describe its main features. During film growth, the triangular defects act as traps for the Cu adatoms while being covered with the A-type O/Cu structure. Initially, the defects are populated by Cu atoms, thus appearing as small triangular islands, instead of triangular defects, within the O/Cu domains [Fig. 5(b)]. The unusual temperature dependence of the island density of the A-type structure is also explained by the defect-induced nucleation. Annealing the films causes the density of the triangular defects to increase at the cost of the honeycomblike defects.[32] Therefore, the density of the triangular defects rises with temperature. Consequently, the nucleation density rises with temperature, too.

We now consider the size distribution of the islands. For small Θ_O where only parts of the Cu film surface are covered with the O/Cu structure [see, e.g., Fig. 3(a)], there is a relatively great variety of island sizes. In the central part of the O/Cu domains, usually, larger islands are found which are surrounded by smaller ones. Obviously, the larger Cu islands are formed by coalescence of smaller islands. This means, the larger islands represent an advanced stage after nucleation, whereas the smaller ones correspond to a stage just after nucleation. Considering also that the small islands are free of O, we conclude that the A-type O/Cu structure is rather mobile. Obviously, it is laterally displaced by the growing Cu islands, which induces a new nucleation around the larger islands. Therefore, nucleation together with the O/Cu domains spreads over formerly O-free Cu terraces. As a consequence, for the A-type structure nucleation and coalescence may simultaneously proceed during film growth. Since the O/Cu domains only occur on larger islands, we assume that the O/Cu structure migrates to the top level of the film before the islands coalesce in the central parts of the O/Cu domains. Probably, the O/Cu structure is pushed on top when it is compressed between growing islands. The mechanism of the lateral and the vertical O/Cu migration, however, is unknown. So far, we cannot decide whether individual O atoms, molecules of O-Cu compounds, or even whole complexes of the O/Cu structure are transferred.

We now turn to the main surfactant effect, i.e., the O-induced layer-by-layer growth observed for $0.2 \leq \Theta_O \leq 0.4$ ML. Obviously, the interlayer diffusion is increased by the O/Cu structure. For the A-type structure, it is most important that small islands are always free of O. Therefore, the diffusion of the Cu adatoms on top of the islands should not initially be affected by O. Consequently, two different diffusion lengths of Cu adatoms have to be considered. The diffusion length within the O/Cu structure is

short, as the high nucleation density indicates. On top of the O-free islands, the diffusion length is relatively large, similarly to that of the clean Cu film. Hence, the adatoms are visiting step sites with a high frequency, so that the number of attempts the adatoms on top of the islands have for step descent is drastically increased compared to clean Cu films. Therefore, the interlayer diffusion is intensified, resulting in 2D island growth. Before the coalescence of the initially clean Cu islands, the O/Cu structure migrates on top, again causing a large density of nuclei on the newly formed layer. Thus, the situation is very much in line with the model of surfactant-mediated film growth recently described by Rosenfeld, Poelsema, and Comsa.[1] They also assume a low adatom mobility during nucleation and a high adatom mobility on top of the small islands.

For small Θ_O [Fig. 3(a)], the O/Cu structure forms separate domains. Here it becomes evident that the 2D film growth also presupposes the lateral displacement of the O/Cu structure. The lateral movement of the O/Cu domains during the 2D growth of the Cu islands enables the O-induced 2D nucleation to spread over the entire surface. Hence both effects, i.e., the retarded formation of the O/Cu structure on top of the islands (it prevents the nucleation on top of already grown 2D Cu islands), and the lateral displacement of the O/Cu structure (it induces the island formation on formerly O-free areas) explain the 2D film growth established for $0.2 \leqslant \Theta_O \leqslant 0.4$ ML.

At $0.1 < \Theta_O < 0.2$ ML, the growth mode is different. Here, the O/Cu structure forms isolated domains, which remain separated during the Cu film growth. Within the O/Cu domains, nucleation, growth, and coalescence of small Cu islands proceeds locally. The small islands coalesce, resulting in large islands, on top of which the O/Cu structure migrates. There the process of locally restricted O-induced nucleation periodically repeats. As a result, multilayer growth is induced, where the top terraces are decorated with 2D islands, and the lower terraces spread by step flow (Fig. 2). This type of multilayer growth is different from that of the clean Cu/Ru(0001) system. It is induced not only by a high step-edge barrier but also by the local restriction of the O-induced nucleation. The latter most effectively traps the Cu adatoms on top of islands, thus also reducing the interlayer diffusion.

Finally, we consider the shape of the Cu islands. Within the A-type O/Cu structure, the islands are always triangular in shape, with steps parallel to atomically closed-packed [110]-like directions [Figs. 3(a), 3(b), 5(a), and 5(b)]. The A-type O/Cu structure is always found on the lower side of the [110]-like steps, with the upper side being free of O. Along the [110]-like steps, the O/Cu structure shows a special configuration, with the step edges appearing like a sawtooth [Fig. 5(a), see arrow]. Obviously, this special O/Cu configuration drastically reduces the energy of [110]-like step edges. The latter can be considered as the driving force in the promotion of the morphology of triangular islands. For {111} surfaces of fcc crystals there are two types of [110]-like steps. They are either of {100} type, or of {111} type. Our investigations indicate that only one type of [110]-like step prevails. If both step types had formed, hexagonal islands instead of triangular ones should have been observed. Up to now, we do not know which type of [110]-like step is favored. The O-atom configuration at the steps may be informative in this respect. High-resolution STM images show the O-induced depressions on the lower side of the [110]-like steps [Fig. 2(c)]. Recently, for Pt(111), it has been shown that O is adsorbed on the lower side of the {100} steps, whereas, for {111} steps, it is on the upper side.[41] Provided this relation holds also for our system, we have to conclude that O most probably stabilizes the {100} steps of Cu.

C. Growth for $0.4 < \Theta_O \leqslant 0.5$ ML

We now turn to the growth effects induced by the B-type O/Cu structure. As mentioned above, the B-type structure completely covers the surface. Even small islands and island edges always display the same corrugation pattern as large terraces do. Obviously, the B-type O/Cu structure immediately forms on top of newly formed islands. The experiments reveal a strong temperature dependence of the Cu nucleation induced by the B-type structure, which is demonstrated by the Arrhenius plot of Fig. 8. Unlike the A-type structure, there is no correlation between the nucleation and the defects belonging to the moiré-like reconstruction of the Cu film. As the B-type O/Cu structure is not interrupted at the defects, it can be considered as a continuous layer bridging Cu defect sites. Regarding the Cu adatom diffusion, generally, there are three possibilities: Cu adatoms may diffuse (i) on top of the O/Cu layer, (ii) within it or (iii) below it. Our oxide model developed for the O/Cu structure[39] implies strong ionic bonds between O and Cu atoms. Hence, we eliminate possibility (ii), since it presupposes breaking of these bonds. Possibility (iii) we exclude also because then the nucleation would be influenced by defects of the Cu film below the O/Cu layer, which was not observed for the B-type structure. Therefore, (i) is the most favorable case. The adatoms may easily migrate on top of the O/Cu layer, where most of the ionic bonds are saturated. Occasionally, the adatoms may penetrate the O/Cu layer in order to form nuclei or to be incorporated at step sites. In order to understand the Arrhenius-like temperature dependence of nucleation, we assume specific diffusion barriers on top of the B-type O/Cu layer, which induce a homogeneous nucleation of Cu adatoms. Correspondingly, we also assume specific additional step-edge barriers. Following nucleation theory,[10,11] and assuming the simplest case, with the dimer being the stable nucleus, the diffusion barrier E_d can be estimated from nucleation density N via $E_d = 3kT \ln(N)$, where k is the Boltzmann factor, and T is the absolute temperature. The fit to our measurements yields $E_d \sim 0.9$ eV, which is more than one order of magnitude higher than the diffusion barrier of the clean Cu(111) surface. Moreover, the additional step-edge barrier Δ_s can roughly be estimated by Eq. (1). In order to obtain Δ_s, we analyzed Cu films grown on O-saturated Ru(0001) showing the transition from 3D to 2D film growth at a temperature of about 350 K. For the measured Cu island distances $D \approx 110$ nm and the critical island radius $R_1 \approx 50$ nm, at which 2D nucleation starts on top, $\Delta_s = 0.08$ eV is obtained. Comparing this value with that of the clean Cu film, we see that for the B-type O/Cu layer, Δ_s is about 50% smaller. Of course, these results have to be considered with some care. The assumption of the dimer as the smallest stable nucleus is problematic. For clean metals, the dimers may dissociate well below RT.[42] On the other hand,

for surfactant-mediated film growth the situation is quite different and more complex. In particular, for the O/Cu system, the surfactant may even stabilize the dimer. Thermal-desorption spectroscopy proved that O generally reinforces the bonding of Cu atoms.[22,28] Thus, our assumption of the dimer as a stable nucleus is not unfounded. Moreover, it is sustained by the absence of bends in the linear slope of the Arrhenius plot of Fig. 8.[43] Nevertheless, we have to emphasize that the atomic configurations defining the diffusion barriers at the O/Cu layer may entirely differ from those of the clean Cu(111) surface. As a consequence, the diffusion barriers obtained for the O/Cu structure do not directly correlate to the barriers of clean Cu(111).

The relatively small additional step-edge barrier found for the B-type structure implies a strong increase of the interlayer diffusion. Hence, it immediately explains the layer-by-layer growth observed at temperatures around 400 K. The alternative model based on the concept of two mobilities[1] (low adatom mobility during nucleation on terraces and high adatom mobility on top of the islands) is clearly not applicable to the B-type O/Cu structure. Since small islands as well as large terraces always show the same O/Cu corrugation pattern, there is no reason to assume different mobilities at any stage of film growth.

At first glance, the B-type O/Cu structure seems to induce effects similar to those observed for Sb-mediated Ag(111) homoepitaxy. There also quite a large diffusion barrier and a rather small additional step-edge barrier were deduced from the experiments.[7] Nevertheless, we assume different surfactant mechanisms. The Sb-mediated Ag homoepitaxy works with relatively small Sb coverages (0.08 ML). Therefore, the idea of a continuous surfactant layer is inappropriate for the Sb/Ag(111) system. The Sb atoms are assumed to exist as interstitials in the surface,[44] where they may act as repulsive centers for Ag adatoms,[14,45] thus increasing the diffusion barrier E_d. Presupposing that the step-edge barrier E_s remains unchanged,[7,15] the latter implies a strong decrease of Δ_s.

Finally, we discuss how our STM investigations correlate with previous measurements of work-function changes performed during film growth.[17] In principle, they confirm the previous measurements and their interpretation. The O-induced 2D film growth deduced from the integral work-function oscillations, was directly evidenced by microscopic real-space imaging. However, the work-function oscillations revealed only a special type of layer-by-layer growth, found for $\Theta_O \approx 0.4$ ML, where STM yielded an extremely high density of 2D nuclei induced by the A-type O/Cu structure. As a matter of fact, the sensitivity of the work-function method to identifying growth modes is rather restricted. The work-function changes attributed to variations in the island density (and thus in the step density) can be explained by the Smoluchowski effect.[17,46] The dipoles occurring at steps reduce the work function. According to our observations, O atoms are located on the lower step sides. They possibly amplify the Smoluchowski dipole due to their high electronegativity. Because of the preferred localization of the dipoles at steps, measurable changes of the work function require a high density of step sites. Even the maximum density of steps and islands, we found in our STM investigations, can probably not describe the oscillations in the work function previously observed. There is one difference between our STM experiments and the previous work-function measurements that should always be taken into account. While the STM measurements are performed after Cu deposition, the work-function oscillations are measured *in situ* (e.g., during evaporation). After the Cu deposition is stopped, the work function increases to almost the same constant value after several seconds, independently of growth stage, as reported in Ref. 17. The final work-function rise may have two explanations. (i) It might be caused by the retarded flow out of the A-type O/Cu structure on top of the growing Cu islands. The latter may predominantly occur after evaporation is stopped (i.e., during Cu film growth the islands are covered with fewer O/Cu areas than observed by STM). (ii) The work-function rise can be attributed to a possible change in the film morphology. During film growth, a dendritic or fractal island morphology may be established, with an extremely high density of step sites. At the end of evaporation, a fast step-edge diffusion may quickly change the dendritic morphology into regular triangular islands, revealed by STM. This reduction in step sites is accompanied by a final rise in the work function.

V. SUMMARY

STM was used to investigate the growth of Cu films on clean and O-precovered Ru(0001), respectively, revealing drastic differences in the growth behavior. Within the range of temperatures analyzed (300–450 K), clean Cu films show a multilayer growth, resulting in a 3D film morphology. In general, the density of nuclei is relatively low, due to the high mobility of Cu adatoms on clean Cu(111) and on Ru(0001). At high resolution, a characteristic defect pattern is revealed belonging to the moiré-like relaxation of the Cu film.

Precovering the Ru(0001) substrate with O modifies the Cu film growth. At $\Theta_O \approx 0.1$ ML, O starts to appear in the Cu film surface and acts as a surfactant. Two different O/Cu surfactant structures (A-type and B-type) were identified that differ in their surfactant mechanisms. The A-type O/Cu structure occurring at $0.1 < \Theta_O \leq 0.4$ ML forms domains, the lateral extension of which increases with Θ_O. Locally, it displays some order, inducing a large density of Cu islands, which slightly increases with temperature. A heterogeneous nucleation is caused by the defects of the moiré-like relaxation of the Cu film. The Cu islands are of triangular shape, with steps parallel to closed-packed [110]-like directions. Small islands are generally free of O. The diffusion length of the Cu adatoms on top of the islands is larger than that within the O/Cu domains, the nucleation density of which is high. Consequently, the number of attempts the atoms have to jump down the steps is increased, which enhances interlayer diffusion. For $0.2 < \Theta_O \leq 0.4$ ML, the latter induces an almost perfect layer-by-layer growth at temperatures around 400 K.

The B-type structure occurring at $0.4 < \Theta_O \leq 0.5$ ML completely covers the Cu film surface. It shows a somewhat lower degree of ordering. The Cu islands formed within the B-type structure are of irregular shape. Their density strongly decreases with rising temperature. 3D multilayer growth, almost perfect layer-by-layer growth, and step flow are observed, with the temperature rising. The B-type structure

forms a continuous layer that bridges the defects of the Cu film. We presuppose that the Cu adatoms diffuse on top of the O/Cu layer and occasionally penetrate it in order to form nuclei or to be incorporated at the step sites. Homogeneous nucleation is assumed for the *B*-type O/Cu layer. Its surfactant effect is ascribed to a relatively large diffusion barrier and a relatively low additional step-edge barrier, established for Cu adatoms on top of the O/Cu layer.

The STM investigations confirm the previous picture of the O-mediated layer-by-layer growth that was deduced from work-function oscillations. However, the data acquisition for STM is delayed in contrast to the work-function measurements that were performed *in situ* during metal deposition. The film morphology measured by STM may be affected by a possible restructuring of the Cu films (e.g., step smoothing), occurring shortly after the evaporation is stopped.

ACKNOWLEDGMENTS

This work was supported by the Deutsche Forschungsgemeinschaft. K.M. and Ch. A. gratefully acknowledge the support by the Max-Planck-Gesellschaft zur Förderung der Wissenschaften, and H.W. is grateful to the Kultusministerium des Landes Sachsen-Anhalt.

[1] G. Rosenfeld, B. Poelsema, and G. Comsa, J. Cryst. Growth **151**, 230 (1995).

[2] W. Wulfhekel, N. N. Lipkin, J. Kliewer, G. Rosenfeld, L. C. Jorritsma, B. Poelsema, and G. Comsa, Surf. Sci. **348**, 227 (1996).

[3] R. L. Schwoebel and E. J. Shipsey, J. Appl. Phys. **37**, 3682 (1966).

[4] G. Ehrlich and F. G. Hudda, J. Chem. Phys. **44**, 1039 (1966).

[5] K. Meinel, M. Klaua, and H. Bethge, J. Cryst. Growth **89**, 447 (1988).

[6] R. Kunkel, B. Poelsema, L. K. Verheij, and G. Comsa, Phys. Rev. Lett. **65**, 733 (1990).

[7] J. A. Meyer, J. Vrijmoeth, H. A. van der Vegt, E. Vlieg, and R. J. Behm, Phys. Rev. B **51**, 14 790 (1995).

[8] V. A. Markov, O. P. Pchelyakov, L. V. Sokolov, S. I. Stenin, and S. Stenin, Surf. Sci. **250**, 229 (1991).

[9] G. Rosenfeld, R. Servaty, C. Teichert, B. Poelsema, and G. Comsa, Phys. Rev. Lett. **71**, 895 (1993).

[10] J. A. Venables, Philos. Mag. **27**, 697 (1973).

[11] J. A. Venables, G. D. T. Spiller, and M. Hanbücken, Rep. Prog. Phys. **47**, 399 (1984).

[12] W. F. Egelhoff, Jr. and D. A. Steigerwald, J. Vac. Sci. Technol. A **7**, 2167 (1989).

[13] H. A. van der Vegt, H. M. van Pinxteren, M. Lohmeier, and E. Vlieg, Phys. Rev. Lett. **68**, 3335 (1992).

[14] S. Oppo, V. Fiorentini, and M. Scheffler, Phys. Rev. Lett. **71**, 2437 (1993).

[15] J. Vrijmoeth, H. A. van der Vegt, J. A. Meyer, E. Vlieg, and R. J. Behm, Phys. Rev. Lett. **72**, 3843 (1994).

[16] S. Esch, M. Hohage, Th. Michely, and G. Comsa, Phys. Rev. Lett. **72**, 518 (1994).

[17] H. Wolter, M. Schmidt, and K. Wandelt, Surf. Sci. **29**, 8173 (1993).

[18] M. Nohlen, M. Schmidt, and K. Wandelt, Surf. Sci. **331–333**, 902 (1995).

[19] C. Park, E. Bauer, and H. Poppa, Surf. Sci. **187**, 86 (1987).

[20] C. Günther, J. Vrijmoeth, R. Q. Hwang, and R. J. Behm, Phys. Rev. Lett. **74**, 754 (1995).

[21] Ch. Ammer, K. Meinel, H. Wolter, A. Beckmann, and H. Neddermeyer, Surf. Sci. **375**, 302 (1997).

[22] K. Kalki, M. Schick, G. Ceballos, and K. Wandelt, Thin Solid Films **228**, 36 (1993).

[23] Y. G. Shen, D. J. O'Connor, H. van Zee, K. Wandelt, and R. J. MacDonald, Thin Solid Films **263**, 72 (1995).

[24] K. Kalki, H. Wang, M. Lohmeier, M. Schick, M. Milun, and K. Wandelt, Surf. Sci. **269–270**, 310 (1992).

[25] R. J. Behm (private communication).

[26] T. E. Madey, H. A. Engelhardt, and D. Menzel, Surf. Sci. **48**, 393 (1975).

[27] Th. Berghaus, A. Brodde, H. Neddermeyer, and St. Tosch, Surf. Sci. **184**, 273 (1987).

[28] K. Kalki, Ph. D. thesis, Universität Bonn, 1992.

[29] H. Pfnür, G. Held, M. Lindroos, and D. Menzel, Surf. Sci. **220**, 43 (1989).

[30] M. Lindroos, H. Pfnür, G. Held, and D. Menzel, Surf. Sci. **222**, 451 (1989).

[31] K. Meinel, H. Wolter, Ch. Ammer, A. Beckmann, and H. Neddermeyer, J. Phys. Condens. Matter **9**, 4611 (1997).

[32] K. Meinel, H. Wolter, Ch. Ammer, and H. Neddermeyer (unpublished).

[33] H. Wolter, K. Meinel, Ch. Ammer, K. Wandelt, and H. Neddermeyer, Surf. Sci. **377–379**, 983 (1997).

[34] Yinggang Li and A. E. De Pristo, Surf. Sci. **319**, 141 (1994).

[35] G. Meyer, J. Wollschläger, and M. Henzler, Surf. Sci. **231**, 64 (1990).

[36] F. Jensen, F. Besenbacher, E. Laegsgaard and I. Steensgaard, Surf. Sci. Lett. **259**, D774 (1991).

[37] D. J. Coulman, J. Winterlin, R. J. Behm, and G. Ertl, Phys. Rev. Lett. **64**, 1761 (1990).

[38] Ch. Ammer, K. Meinel, H. Wolter, and H. Neddermeyer, Surf. Sci. **377–379**, 81 (1997).

[39] Ch. Ammer, K. Meinel, H. Wolter, and H. Neddermeyer (unpublished).

[40] K. Meinel, H. Wolter, Ch. Ammer, and H. Neddermeyer (unpublished).

[41] P. J. Feibelman, S. Esch, and Th. Michely, Phys. Rev. Lett. **77**, 2257 (1996).

[42] H. Röder, E. Hahn, H. Brune, J.-P. Bucher, and K. Kern, Nature (London) **366**, 141 (1993).

[43] H. Brune, K. Bromann, H. Röder, and K. Kern, Phys. Rev. B **52**, R14 380 (1995).

[44] J. A. Meyer, H. A. van der Vegt, J. Vrijmoeth, E. Vlieg, and R. J. Behm, Surf. Sci. Lett. **355**, L375 (1996).

[45] S. Liu, L. Bönig, J. Detch, and H. Metiu, Phys. Rev. Lett. **74**, 4495 (1995).

[46] R. Smoluchowski, Phys. Rev. **60**, 661 (1941).